Pack cementation to prevent the oxidation of CoSb in air at 800 K

Richard Drevet, Lionel Aranda, Nicolas David, Carine Petitjean, Delphine Veys-Renaux, Patrice Berthod

Version of Record: https://www.sciencedirect.com/science/article/pii/S0257897220300700
Manuscript_6a046b3a0de10cad08ba0fc4031401bf

Pack cementation to prevent the oxidation of $CoSb_3$ in air at 800 K

Richard DREVET*, Lionel ARANDA, Nicolas DAVID, Carine PETITJEAN, Delphine VEYS-RENAUX, Patrice BERTHOD

Institut Jean Lamour, CNRS - Université de Lorraine, UMR 7198, Campus Artem, allée André Guinier, BP 50840, 54011 Nancy cedex, France.

* corresponding author.

Tel.: +33.372.74.27.29.

e-mail address: richarddrevet@yahoo.fr

Abstract

The skutterudite $CoSb_3$ is a well-known thermoelectric material widely used to produce electricity from heat. This material is commonly employed under vacuum but in a near future it is expected to be used at high temperatures under oxidative atmospheres, e.g. in air. The lifetime of the material may be affected by the oxidative environment, considerably limiting the use of the thermoelectric equipment. The present research describes the degradation mechanisms of $CoSb_3$ from oxidation experiments carried out under a flow of synthetic air at 800 K. The skutterudite material is progressively oxidized after 15 h, 50 h, 100 h and 1000 h of treatment, producing three oxides on the $CoSb_3$ surface ($CoSb_2O_4$ / $CoO{\cdot}Sb_2O_3$, Sb_2O_4 and $CoSb_2O_6$). These three oxides have different growth kinetics and they are produced in various amounts as a function of the oxidation time.

Next, as a solution for an appropriate oxidation protection, this work explores the chemical vapor deposition (CVD) process named pack cementation to synthesize a protective coating on $CoSb_3$. This process produces a surface layer made of aluminum antimonide (AlSb) and cobalt aluminide (Al_9Co_2). The oxidation experiments carried out on the coated $CoSb_3$ highlight the protective properties of this innovative surface layer. The coating is a protective barrier against oxygen that keeps the $CoSb_3$ substrate unaffected by the flow of air at 800 K for 1000 hours. Consequently, pack cementation is an efficient process to synthesize a protective surface layer that makes $CoSb_3$ usable under oxidative environments.

Keywords: skutterudite; oxidation; aluminizing; pack cementation; corrosion; thermoelectric material

1. Introduction

The skutterudite materials are widely studied in the academic and industrial research due to their outstanding thermoelectric properties. They are intensively developed to produce thermoelectric generators able to convert the heat flows into electrical energy [**1-3**]. The skutterudite materials made of cobalt and antimony are particularly very attractive because of their high electron mobility, high atomic masses, low electrical resistivity and good Seebeck coefficients [**4-6**]. The most widespread skutterudite material is $CoSb_3$, commonly employed at high temperatures under vacuum in space industry [**7-9**]. This thermoelectric material provides a continuous electrical energy for batteries in satellites and spacecrafts [**10**]. Since they are powerful electrical energy producers, the skutterudite materials are currently considered as an alternative to the use of fossil fuels on Earth [**11-12**]. However, under an oxidizing environment such as air at high temperature, they may degrade progressively in service. Ideally, for potential industrial applications, the skutterudite materials have to withstand 1000 hours of exposure in air at 800 K, a relevant temperature found for example in car exhaust gases [**12-13**]. If this objective is reached, $CoSb_3$ will be considered as an interesting and powerful material to produce innovative electrical generators.

Several research works have described the oxidation behavior of $CoSb_3$ but mainly at temperatures lower than 800 K. Generally, the oxidation of $CoSb_3$ induces the formation of a two-part surface layer made of a mixture of antimony oxides outwards and made of a mixture of antimony oxides and cobalt antimonates inwards [**14**]. This surface layer grows according to a parabolic thickness-time dependence. The growth mechanism occurs in three steps: (i) antimony segregation on the surface, (ii) oxygen penetration into the region of antimony segregation, and (iii) reaction [**15**]. This oxidation behavior degrades the thermoelectric properties of $CoSb_3$ and the electrical device durability [**16**].

In order to lower the impact of oxidation in air at high temperatures, several coating processes have been studied in literature such as magnetron-sputtering or sol-gel process [**17-19**]. The chemical vapor deposition (CVD) process named pack cementation is well-known to produce protective coatings made of aluminum at the surface of metallic materials [**20-22**]. Recently we have explored the isothermal section at 600°C of the Al-Co-Sb ternary system to point out the thermodynamic stability of several phases of aluminum and antimony or aluminum and cobalt [**23**]. These results highlight the relevance of using aluminum pack cementation to produce a surface coating on the skutterudite material $CoSb_3$. To assess the protection provided by the synthesized surface layer, the current research describes the oxidation behavior of both uncoated and coated $CoSb_3$ samples under a flow of synthetic air at 800 K for 1000 hours.

2. Materials and Methods

2.1. Synthesis of the skutterudite materials

The $CoSb_3$ polycrystalline samples were obtained by melting stoichiometric amounts of high purity cobalt (Co, 99.99 %) and antimony (Sb, 99.999 %) at 1373 K for 24 hours in a vitreous-carbon crucible sealed in a quartz tube under partial argon atmosphere. The skutterudite phase is obtained in a second step by cooling down the temperature at 1073 K for a constant annealing for four days. Then, the sample was thoroughly crushed in an agate mortar and the obtained powder is sieved at 36 µm. At last this powder is densified by spark plasma sintering (SPS, Syntex DR SINTER Lab 515S) in graphite dies for 10 minutes at 893 K under 50 MPa. This protocol produces cylindrical samples of 10 mm in diameter and 2 mm in height [**24-25**].

2.2. Preparation and oxidation of the skutterudite materials

The $CoSb_3$ skutterudite samples were slightly polished with a 1200 grit SiC paper to remove the surface impurities and ultrasonically cleaned in ethanol. Next, the oxidation of the samples was carried out in a tubular furnace (Carbolite) in which a flow (4 L h^{-1}) of synthetic air, i.e. a mixture of dioxygen (20 % O_2) and dinitrogen (80 % N_2), is continuously injected. The studied temperature to oxidize the samples was 800 K applied for 15 h, 50 h, 100 h and 1000 h.

2.3. Synthesis of the coating

The chemical vapor deposition (CVD) process used to coat the $CoSb_3$ substrate was pack cementation. Firstly, the surface of the $CoSb_3$ pellet was polished with a 1200 grit SiC papers and ultrasonically cleaned in ethanol. Then, the pellet was positioned under a dynamic secondary vacuum (10^{-6} mbar) inside a sealed silica ampoule that contained a mixture of three powders : 0.60 g of Al (the element to be deposited), 1.40 g of Al_2O_3 (the inert filler powder) and 0.02 g of $CrCl_3$ (the halide salt activator). These amounts correspond to 0.92 g of powder per cm^2 of surface of the $CoSb_3$ sample. The ampoule was annealed in a muffle furnace (Nabertherm) by increasing the temperature with a heating rate of 10 K min^{-1} until 873 K for 30 min or until 773 K for 120 min. At these temperatures, the atomic diffusions produces a surface layer made of aluminum combined to atoms from the substrate [**20-22**]. At last, the silica ampoule was air-quenched at room temperature.

2.4. Characterization of the skutterudite materials

The mass variation (Δm) of the oxidized samples was measured with a precision balance (METTLER-TOLEDO). The surface morphology of the samples was observed from secondary

electron (SE) images obtained with a scanning electron microscope (SEM, JEOL JSM 6010LA). The cross-sections were observed from backscattered electron (BSE) images. Moreover, energy dispersive X-ray spectroscopy (EDS) was used to identify the chemical elements inside the surface layer of the oxidized samples and to quantify them from the resulting X-ray microanalysis. In order to get a representative value of these quantifications, three EDS spots were acquired on the whole thickness of the surface layers observed from the cross-section images. The presented values correspond to the average of these triplicate measurements. The crystalline phases of the samples were characterized by X-ray diffraction (XRD) with a Philips X'pert Pro diffractometer using a monochromatic $Cu_{K\alpha}$ radiation ($\lambda = 0.15406$ nm). The patterns were collected from $2\theta = 20°$ to 60° with a step of 0.033°. The phases were identified from the diffraction files provided by the International Centre for Diffraction Data (ICDD).

3. Results and discussion

3.1. Oxidation of the $CoSb_3$ skutterudite material

The $CoSb_3$ material has been oxidized under a flow of synthetic air at 800 K for 15 h, 50 h, 100 h and 1000 h. The corresponding surface modifications are presented on the SEM images of **Fig.1**. These SEM observations display the progressive growth of a surface layer with the oxidation time. The cross-section BSE-SEM images of **Fig.2** highlight this surface layer whose thickness increases until 1000 hours of treatment. After 15 h and 50 h of oxidation, only one contrast is noticeable in the newly formed layer. After 100 h and 1000 h of oxidation, several contrasts are clearly visible inside the surface layer, indicating the presence of several different phases [**26-27**]. The corresponding mass and thickness variations are plotted in **Fig.3**. We can see on these curves that both parameters increase quickly until 100 hours of oxidation. Next, although the thickness of the

layer is still increasing until 1000 hours of oxidation, the mass variation slightly decreases after 1000 hours in comparison with that measured after 100 h of oxidation. In order to understand the oxide layer growth mechanism, the 100 hours oxidation experiment has been reiterated on another $CoSb_3$ substrate the surface of which has been previously covered by a few nanometers thick gold layer deposited by evaporation process. During the thermal treatment at 800 K, this thin gold layer forms numerous small agglomerates on the surface, clearly observable in white on the cross-section BSE-SEM images of **Fig.4**. The two parts of the surface layer formed during the oxidation treatment are evidently distinguishable on the BSE-SEM images. Their chemical analyzes are carried out from pointed EDS spectra and the corresponding elemental quantifications are reported in **Table 1**. The lower part has grown towards the inside of the $CoSb_3$ substrate and it is made of oxygen, cobalt and antimony. The upper part has grown towards the outside of the $CoSb_3$ substrate and it is only made of oxygen and antimony. According to the XRD patterns of **Fig.5**, this oxide layer is mainly composed of the spinel $CoSb_2O_4$ / $CoO{\cdot}Sb_2O_3$, always the major phase whatever the duration of oxidation. From 100 hours of oxidation, Sb_2O_4 appears on the XRD patterns that corresponds to the upper part of the surface oxide layer identified by EDS from the cross-section images of **Fig.2** and **Fig.4**. The oxide Sb_2O_4 is known to be a reaction product obtained in two steps from the unstable oxide Sb_2O_3 according to reaction (1) and reaction (2) [**28-29**]:

$$4\ CoSb_3\ (s) + 11\ O_2\ (g) \rightarrow 4\ CoSb_2O_4\ (s) + 2\ Sb_2O_3\ (s) \qquad (1)$$

$$4\ Sb_2O_3\ (s) \rightarrow 2/n\ Sb_n\ (g) + 3\ Sb_2O_4\ (s) \qquad (2)$$

The solid oxidation products Sb_2O_4 (s) is formed at the surface of the oxidized $CoSb_3$ together with volatile species evaporated just after being formed [**29-30**]. The more Sb_2O_4 (s) is formed, the more

some elements from the substrate are evaporated. These oxidation reactions explain why the mass variation decreases after 1000 hours of oxidation whereas the oxide layer thickness is still increasing at the surface of the $CoSb_3$ substrate. At last, the XRD patterns reveal that another oxide ($CoSb_2O_6$) starts to appear from 100 hours of treatment and becomes clearly noticeable after 1000 hours of oxidation. This phase is positioned at the interface between the two oxides previously presented ($CoSb_2O_4$ / $CoO{\cdot}Sb_2O_3$ and Sb_2O_4). The formation of $CoSb_2O_6$ takes place after reaction (1) according to reaction (3) [**30-31**]:

$$CoSb_2O_4\ (s) + O_2\ (g) \rightarrow CoSb_2O_6\ (s) \qquad (3)$$

This reaction suggests that some oxygen diffuses through the upper oxide layer (Sb_2O_4) to reach the lower oxide layer ($CoSb_2O_4$) to react with it. Another explanation provided by Godlewska *et al.* indicates that the phase $CoSb_2O_6$ appears at the later stages of the oxidation process as a result of a secondary reaction between Sb_2O_4 and $CoSb_2O_4$ at their interface [**28**].

Consequently, these results clearly highlight the degradation of the $CoSb_3$ material under a flow of air at 800 K. The surface protection of this material is essential for any industrial applications in air.

3.2. Aluminizing of the $CoSb_3$ skutterudite material

The CVD process named pack cementation is used to aluminize two $CoSb_3$ substrates in two different experimental conditions, one at 773 K for 120 minutes and the other one at 873 K for 30 minutes. The mass of both $CoSb_3$ samples increases during the deposition process, $\Delta m = +0.86$ mg cm^{-2} and $\Delta m = +1.37$ mg cm^{-2}, respectively. The corresponding surface morphologies obtained after deposition are observed on the SEM images of **Fig.6**. In both cases, a dense rough layer is

produced at the surface of the $CoSb_3$ substrate. Indeed, during the pack cementation process, the coating is synthesized by atomic diffusions at the surface of the $CoSb_3$ substrate. The aluminum atoms react with cobalt and antimony atoms to produce a coating at the surface of the material, keeping the initial topography of the substrate [**20-22**]. The cross-section BSE-SEM images of **Fig.7** and **Fig.8** indicate that the thickness of the coatings is 8 µm and 13 µm, respectively. The X-ray maps and the EDS spectra show that these surface coatings are made of aluminum, cobalt and antimony. The corresponding elemental quantifications are reported in **Table 1**. Both samples show higher amounts of aluminum at the upper part of the coating (spectrum #1) than at the interface with the substrate (spectrum #2). Cobalt is homogeneously distributed inside the coating whereas the amount of antimony is more important close to the substrate. This behavior may suggest that antimony has formed volatile halides by reacting with the halide salt activator present in the pack ($CrCl_3$) [**21**]. The EDS analyzes carried out inside the substrates are homogeneous with characteristic quantifications of $CoSb_3$. The XRD patterns of **Fig.9** reveal that the two synthetized coatings are similarly composed of two crystalline phases. In both cases, the phase AlSb is the major one and the phase Al_9Co_2 is the minor one. From a thermodynamic point of view, the occurrence of only binary phases without any ternary phase has been justified by the description of the diffusion pathway of Al inside $CoSb_3$ on the isothermal section of the Al-Co-Sb ternary system [**23**]. Moreover, the isothermal section shows that the thermodynamic equilibrium exists between AlSb and $CoSb_3$ justifying why AlSb is firstly formed during the pack cementation process. As well, the thermodynamic equilibrium also exists between AlSb and Al_9Co_2 but with no possible equilibrium between Al_9Co_2 and $CoSb_3$ [**23**]. This assumption means that the formation of Al_9Co_2 occurs during a second step only inside the AlSb layer with no contact with $CoSb_3$. These thermodynamics information implies that during the process the aluminum atoms enter the $CoSb_3$ structure and firstly react with antimony to form AlSb. This reaction induces the formation of

intermediate compounds such as $CoSb_2$ or CoSb that progressively insulate cobalt in the structure. Then, during a second step, cobalt inside the surface layer reacts with aluminum to produce Al_9Co_2 certainly promoted by some intermediate compounds such as AlCo, Al_5Co_2, Al_3Co, $Al_{13}Co_4$ [**23**]. Nonetheless, the amount of Al_9Co_2 is very low and hardly distinguishable from the cross-section BSE-SEM images of **Fig.7** and **Fig.8** although the XRD pattens of **Fig.9** evidence it inside the surface layer. Then, the pack cementation process is a powerful process to produce a surface coating on $CoSb_3$ the protection properties of which have to be assessed from oxidation experiments.

3.3. Oxidation of the aluminized $CoSb_3$ skutterudite materials

The results presented in **Fig.10** and **Fig.11** show the cross-section SEM images of the aluminized $CoSb_3$ substrates after oxidation under a flow of synthetic air at 800 K for 1000 h. The thickness of the surface layer of $CoSb_3$ aluminized at 773 K increases from 8 µm to 12 µm during the oxidation treatment at 800 K (**Fig.10**). The corresponding mass variation is $\Delta m = + 0.05$ mg cm^{-2}. This behavior suggests that the aluminum diffusion continues during the oxidation at 800 K, a temperature upper than that used to aluminize this $CoSb_3$ sample. On the other hand the thickness of the surface layer of $CoSb_3$ aluminized at 873 K remains constant during the oxidation treatment at 800 K (**Fig.11**) but this sample shows a higher mass variation $\Delta m = + 0.19$ mg cm^{-2}. The different behaviors observed for both samples can be attributed to the two different temperatures used for the pack cementation process that induce two different surface layer thicknesses. The X-ray maps and EDS spectra indicate that these two surface layers are made of oxygen, aluminum, cobalt and antimony. The quantitative analyzes of these four elements are reported in **Table 1**. For both samples, the amounts of oxygen and aluminum are higher in the upper part of the coating (spectrum #1) in comparison with the area close to the interface with the substrate (spectrum #2). The amount

of cobalt is low but homogeneously distributed inside the coating whereas the amount of antimony is higher in the area close to the substrate in comparison with the top area of the coating. The EDS analyzes carried out inside the substrates are homogeneous with characteristic quantifications of $CoSb_3$. The X-ray maps show that the whole thickness of the coatings are oxidized with no oxygen detected inside the $CoSb_3$ substrates. These results highlight the great affinity of the surface layer with oxygen, meaning that the synthesized coating is an efficient barrier against oxygen diffusion that provides an appropriate oxidation protection to $CoSb_3$. The corresponding XRD patterns are displayed in **Fig.12**. The signal from AlSb, the main crystalline phase of the coating, is still observable after 1000 h of oxidation at 800 K. However, both XRD patterns include the signal from the $CoSb_3$ substrate, even for the sample whose surface layer thickness has increased during the oxidation treatment. This observation means that the incident X-rays beam penetrates more deeply the sample certainly because the density of the surface layer has been lowered by the oxidation process [**32-33**]. The XRD patterns also highlight that no structural change of $CoSb_3$ occurs during the treatment. On the other hand, one of the oxidized samples also reveal the presence of some alumina (α-Al_2O_3) meaning that a portion of the formed oxides has been crystallized (**Fig.12b**). The corresponding signal is quite low although oxygen is homogeneously distributed on the X-ray maps of **Fig.10** and **Fig.11** with an average amount upper than 40 at.% (**Table 1**). Indeed, the main crystalline phase of the surface layer is AlSb constituted by aluminum and antimony, two chemical elements particularly well-known for their high affinity with oxygen [**34-35**]. Sherohman *et al.* have described the oxidation process of AlSb in air in two steps [**36**]: an initial rapid formation of an oxidized amorphous layer, followed by the continuous oxidation throughout the AlSb material that produces Al_2O_3 and Sb_2O_3 according to reaction (4):

$$2\ AlSb\ (s) + 3\ O_2\ (g) \rightarrow Al_2O_3\ (s) + Sb_2O_3\ (s) \quad (4)$$

Any deviation from stoichiometry brought by non-equivalent oxidation would produce some Al or Sb. They may promote the formation of hydroxide or hydride compounds such as $Al(OH)_3$ or SbH_3 that are known for their instability at high temperatures [**37-38**]. These compounds are easily decomposed from 500 K, producing aluminum oxides (Al_2O_3) and antimony oxides (Sb_2O_3, Sb_2O_4, and Sb_2O_5) [**39-41**]. The volatilization of these unstable compounds can occur during the oxidation treatment, inducing the disruption of the oxidized layer [**42**]. In our experiments the mechanical stability of the layer is preserved during the oxidation treatment but longer oxidation durations may partially destroy the surface layer [**2**].

However, out experimental results have clearly evidenced the protection property of the synthesized biphasic coating under air environment at 800 K for 1000 h. The aluminized surface layer acts as a protecting barrier for the $CoSb_3$ skutterudite material, avoiding any oxygen penetration. The initially targeted objective is then accomplished, making this innovative system interesting and a potential powerful energy producer for many industrial applications.

4. Conclusions

The present research has explored the oxidation behavior of the skutterudite material $CoSb_3$ under a flow of air at 800 K for 15 h, 50 h, 100 h and 1000 h. The growth of a surface oxide layer has been observed for 1000 h of treatment. This oxide layer is made of three phases. The spinel oxide $CoSb_2O_4$ / $CoO{\cdot}Sb_2O_3$ grows inwards the substrate and the two oxides Sb_2O_4 and $CoSb_2O_6$ grow outwards the substrate. In order to prevent the oxidation of $CoSb_3$, a protective surface coating has been synthesized by the CVD process named aluminum pack cementation. The synthesis has been

experimented in two conditions, one at 873 K for 30 min or another one at 773 K for 120 min. In both conditions, the obtained biphasic coating is made of AlSb and Al_9Co_2. The oxidation of the coated $CoSb_3$ under a flow of air at 800 K for 1000 hours has demonstrated the protection properties of this innovative coating that keeps $CoSb_3$ unaffected by oxygen. Consequently, this coating is a powerful and efficient protection barrier that makes the coated $CoSb_3$ skutterudite material an interesting device usable for industrial applications under oxidizing environments.

Acknowledgements

The French National Research Agency (ANR) is gratefully acknowledged for the financial support of the Nanoskut project (ANR-12-PRGE-0008-01).

5. References

[1] M. Rull-Bravo, A. Moure, J.F. Fernandez, M. Martin-Gonzalez, Skutterudites as thermoelectric materials: revisited, RSC Adv. 5 (2015) 41653-41667.

[2] R. Drevet, L. Aranda, C. Petitjean, N. David, D. Veys-Renaux, P. Berthod, Oxidation Behavior of the Skutterudite Material $Ce_{0.75}Fe_3CoSb_{12}$, Oxid. Met. 91 (2019) 767-779.

[3] G. Rogl, P. Rogl, Skutterudites, a most promising group of thermoelectric materials, Curr. Opin. Green Sustain. Chem. 4 (2017) 50-57.

[4] R. Guo, X. Wang, B. Huang, 2015. Thermal conductivity of skutterudite $CoSb_3$ from first principles: Substitution and nanoengineering effects. Sci. Rep. 5, 7806.

[5] J.Q. Guo, H.Y. Geng, T. Ochi, S. Suzuki, M. Kikuchi, Y. Yamaguchi, S. Ito, Development of skutterudite thermoelectric materials and modules, J. Electron. Mater. 41 (2012) 1036-1042.

[6] L. Shi, X. Huang, M. Gu, L. Chen, Interfacial structure and stability in Ni/SKD/Ti/Ni skutterudite thermoelements, Surf. Coat. Technol. 285 (2016) 312-317.

[7] S. Zhang, S. Xu, H. Gao, Q. Lu, T. Lin, P. He, H. Geng, Characterization of multiple-filled skutterudites with high thermoelectric performance, Journal of Alloys and Compounds 814 (2020) article # 152272.

[8] Y. Lei, W. Gao, R. Zheng, Y. Li, R. Wan, W. Chen, L. Ma, H. Zhou, P.K. Chu, Rapid synthesis, microstructure, and thermoelectric properties of skutterudites, Journal of Alloys and Compounds 806 (2019) 537-542.

[9] D. Sivaprahasam, S.B. Chandrasekhar, S. Kashyap, Ashutosh Kumar, R. Gopalan, Thermal conductivity of nanostructured $Fe_{0.04}Co_{0.96}Sb_3$ skutterudite, Materials Letters 252 (2019) 231-234.

[10] W. Liu, Q. Jie, H.S. Kim, Z. Ren, Current progress and future challenges in thermoelectric power generation: From materials to devices, Acta Mater. 87 (2015) 357-376.

[11] L.E. Bell, Colling, heating, generating power, and recovering waste heat with thermoelectric systems, Science 321 (2008) 1457-1461.

[12] V. Andrei, K. Bethke, K. Rademann, Thermoelectricity in the context of renewable energy sources: joining forces instead of competing, Energy Environ. Sci. 9 (2016) 1528-1532.

[13] R. Kühn, O. Koeppen, P. Schulze, D. Jänsch, Comparison between a Plate and a Tube Bundle Geometry of a Simulated Thermoelectric Generator in the Exhaust Gas System of a Vehicle, Mater. Today proc. 2 (2015) 761-769.

[14] V. Savchuk, A. Boulouz, S. Chakraborty, J. Schumann, H. Vinzelberg, Transport and structural properties of binary skutterudite $CoSb_3$ thin films grown by DC magnetron sputtering technique, J. Appl. Phys. 92 (2002) 5319-5326.

[15] R. Hara, S. Inoue, H.T. Kaibe, S. Sano, Aging effect of large-size n-type $CoSb_3$ prepared by spark plasma sintering, J. Alloys Compd 349 (2003) 297-301.

[16] Y.S. Park, T. Thompson, Y. Kim, J.R. Salvador, J.S. Sakamoto, Protective enamel coating for n- and p-type skutterudite thermoelectric materials, J. Mater. Sci. 50 (2015) 1500-1512.

[17] E. Godlewska, K. Zawadzka, K. Mars, R. Mania, K. Wojciechowski, A. Opoka, Protective Properties of Magnetron-Sputtered Cr–Si Layers on $CoSb_3$, Oxid. Met. 74 (2010) 205-213.

[18] D. Zhao, M. Zuo, Z. Wang, X. Teng, H. Geng, Protective properties of magnetron-sputtered Ti coating on $CoSb_3$ thermoelectric material, Appl. Surf. Sci. 305 (2014) 86-92.

[19] H. Dong, X. Li, X. Huang, Y. Zhou, W. Jiang, L. Chen, Improved oxidation resistance of thermoelectric skutterudites coated with composite glass, Ceram. Int. 39 (2013) 4551-4557.

[20] X. Xiang, X. Wang, G. Zhang, T. Tang, X. Lai, Preparation technique and alloying effect of aluminide coatings as tritium permeation barriers : A review, International Journal of Hydrogen Energy 40 (2015) 3697-3707.

[21] R. Mévrel, C. Duret, R. Pichoir, Pack cementation processes, Journal Materials Science and Technology 2 (1986) 201-206.

[22] Z.D. Xiang, P.K. Datta, Relationship between pack chemistry and aluminide coating formation for low-temperature aluminisation of alloy steels, Acta Mater. 54 (2006) 4453-4463.

[23] R. Drevet, C. Petitjean, N. David, L. Aranda, D. Veys-Renaux, P. Berthod, Aluminizing by pack cementation to protect $CoSb_3$ from oxidation, Mater. Chem. Phys. 241 (2020) 122417.

[24] E. Alleno, L. Chen, C. Chubilleau, B. Lenoir, O. Rouleau, M.F. Trichet, B. Villeroy, Thermal Conductivity Reduction in $CoSb_3$-CeO_2 Nanocomposites, J. Electron. Mater. 39 (2010) 1966-1970.

[25] M. Benyahia, V. Ohorodniichuk, E. Leroy, A. Dauscher, B. Lenoir, E. Alleno, High thermoelectric figure of merit in mesostructured $In_{0.25}Co_4Sb_{12}$ *n*-type skutterudite, J. Alloys Compd 735 (2018) 1096-1104.

[26] F. Timischl, N. Inoue, Increasing compositional backscattered electron contrast in scanning electron microscopy, Ultramicroscopy 186 (2018) 82-93.

[27] J. Cazaux, N. Kuwano, K. Sato, Backscattered electron imaging at low emerging angles: A physical approach to contrast in LVSEM, Ultramicroscopy 135 (2013) 43-49.

[28] E. Godlewska, K. Zawadzka, A. Adamczyk, M. Mitoraj, K. Mars, Degradation of $CoSb_3$ in Air at Elevated Temperatures, Oxid. Met. 74 (2010) 113-124.

[29] N.A. Asryan, A.S. Alikhanyan, G.D. Nipan, p-T-x Phase Diagram of the Sb-O System, Inorg. Mater. 40 (2004) 626-631.

[30] J. Leszczynski, K.T. Wojciechowski, A.L. Malecki, Studies on thermal decomposition and oxidation of $CoSb_3$, J. Therm. Anal. Calorim. 105 (2011) 211-222.

[31] K. Zawadzka, E. Godlewska, K. Mars, M. Nocun, A. Kryshtal, A. Czyrska-Filemonowicz, Enhancement of oxidation resistance of $CoSb_3$ thermoelectric material by glass coating, Mater. Des. 119 (2017) 65-75.

[32] L.G. Parratt, Surface Studies of Solids by Total Reflection of X-Rays, Phys. Rev. 95 (1954) 359-369.

[33] Z.H. Kalman, L.A. Johnson, J.B. Wachtman, Density determination of thin coatings by X-ray methods, J. Am. Ceram. Soc. 72 (1989) 1170-1174.

[34] J. Nakata, T. Shibata, Y. Nanishi, M. Fujimoto, Suppression of AlSb oxidation with hydrocarbon passivation layer induced by MeV-He^+ irradiation, J. Appl. Phys. 76 (1994) 2078-2085.

[35] A.J. Rosenberg, The oxidation of intermetallic compounds-III. The room-temperature oxidation of $A^{III}B^{V}$ compounds, J. Phys. Chem. Solids 14 (1960) 175-180.

[36] J.W. Sherohman, J.H. Yee, A.W. Coombs, K.J.J. Wu, 2012. Thermal oxidation of single crystal aluminum antimonide and materials having the same. US Patent Application Publication, US8338916B2.

[37] A.D.V. Souza, C.C. Arruda, L. Fernandes, M.L.P. Antunes, P.K. Kiyohara, R. Salomão, Characterization of aluminum hydroxide ($Al(OH)_3$) for use as a porogenic agent in castable ceramics, J. Europ. Ceram. Soc. 35 (2015) 803-812.

[38] E. Haffer, D. Schmidt, P. Freimann, W. Gerwinski, Simultaneous determination of germanium, arsenic, tin and antimony with total-reflection X-ray fluorescence spectrometry using the hydride generation technique for matrix separation—first steps in the development of a new application, Spectrochim. Acta B 52 (1997) 935-944.

[39] F.W.O. Da Silva, C. Raisin, M. Nouaoura, L. Lassabatère, Auger and electron energy loss spectroscopies study of the oxidation of AlSb(001) thin films grown by molecular beam epitaxy, Thin Solid Films 200 (1991) 33-48.

[40] S. Jakschik, U. Schroeder, T. Hecht, M. Gutsche, H. Seidl, J.W. Bartha, Crystallization behavior of thin ALD-Al_2O_3 films, Thin Solid Films 425 (2003) 216-220.

[41] R.G. Orman, D. Holland, Thermal phase transitions in antimony (III) oxides, J. Solid State Chem. 180 (2007) 2587-2596.

[42] T. Karlsson, C. Forsgren, B.M. Steenari, Recovery of antimony: A laboratory study on the thermal decomposition and carbothermal reduction of Sb(III), Bi(III), Zn(II) oxides, and antimony compounds from metal oxide varistors, J. Sustain. Metall. 4 (2018) 194-204.

Figures caption

Fig.1. SEM images of the $CoSb_3$ surface after oxidation in air at 800 K for (a) 15 h, (b) 50 h, (c) 100 h and (d) 1000 h.

Fig.2. Cross-sections SEM images (BSE) of $CoSb_3$ after oxidation in air at 800 K for (a) 15 h, (b) 50 h, (c) 100 h and (d) 1000 h.

Fig.3. Mass and thickness evolutions of $CoSb_3$ as a function of oxidation time in air at 800 K.

Fig.4. Cross-section SEM image (BSE) and EDS spectra of $CoSb_3$ after oxidation in air at 800 K for 100 h.

Fig.5. XRD patterns of $CoSb_3$ as a function of oxidation time in air at 800 K.

Fig.6. SEM images of the $CoSb_3$ surface after aluminizing by CVD (a) at 773 K for 120 minutes and (b) at 873 K for 30 minutes.

Fig.7. SEM images, EDS characterization and X-ray maps of the cross-section of the $CoSb_3$ surface after aluminizing by CVD at 773 K for 120 minutes.

Fig.8. SEM images, EDS characterization and X-ray maps of the cross-section of the $CoSb_3$ surface after aluminizing by CVD at 873 K for 30 minutes. Reprinted from Ref. [23] with kind permission from Elsevier.

Fig.9. XRD patterns of the $CoSb_3$ surface after aluminizing by CVD (a) at 773 K for 120 minutes and (b) at 873 K for 30 minutes.

Fig.10. SEM images, EDS characterization and X-ray maps of the cross-section obtained after oxidation at 800 K for 1000 hours of $CoSb_3$ aluminized at 773 K for 120 minutes.

Fig.11. SEM images, EDS characterization and X-ray maps of the cross-section obtained after oxidation at 800 K for 1000 hours of $CoSb_3$ aluminized at 873 K for 30 minutes. Reprinted from Ref. [23] with kind permission from Elsevier.

Fig.12. XRD patterns after oxidation at 800 K for 1000 hours of the aluminized $CoSb_3$ surface obtained (a) at 773 K for 120 minutes and (b) at 873 K for 30 minutes.

Fig.1

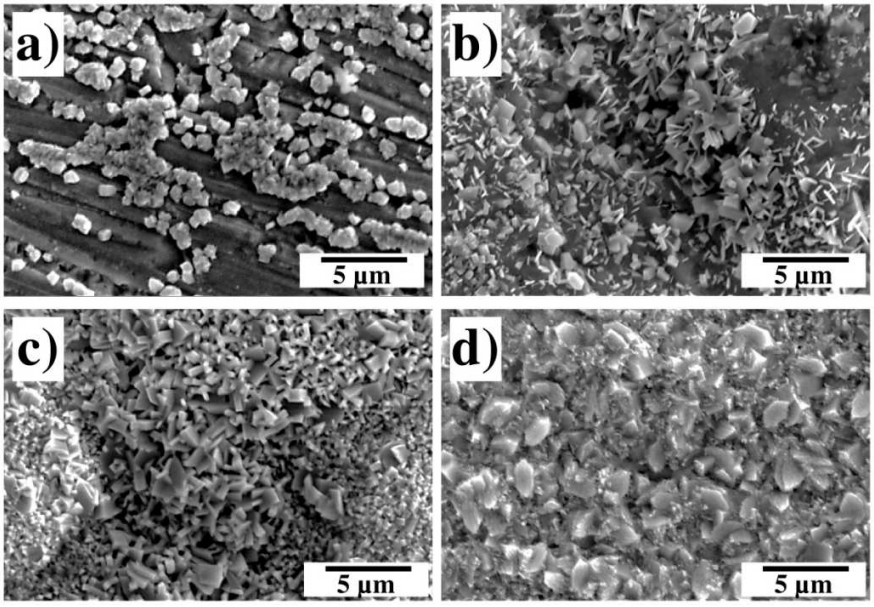

Fig.2

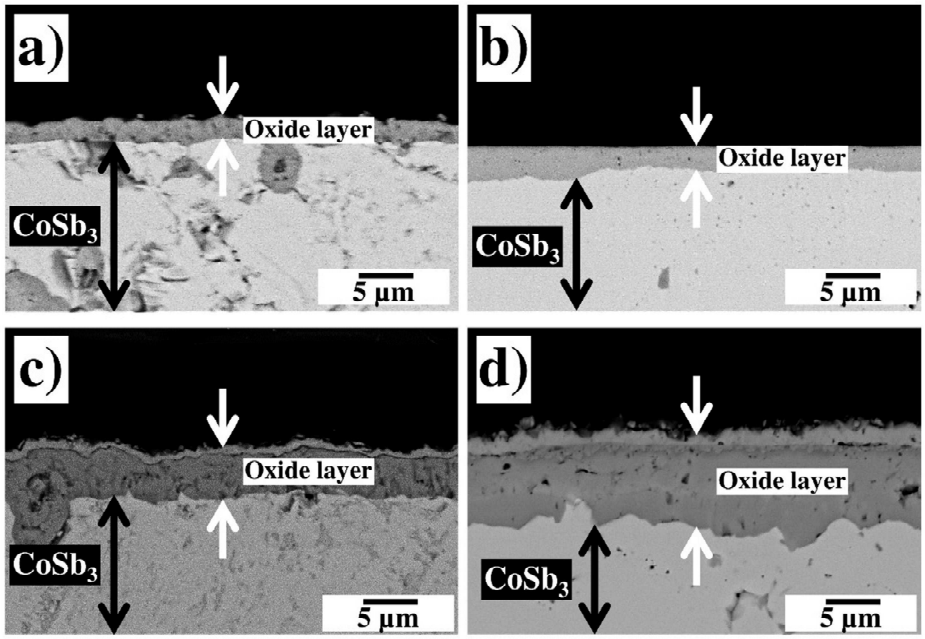
a)
Oxide layer
$CoSb_3$
5 μm
b)
Oxide layer
$CoSb_3$
5 μm
c)
Oxide layer
$CoSb_3$
5 μm
d)
Oxide layer
$CoSb_3$
5 μm

Fig.3

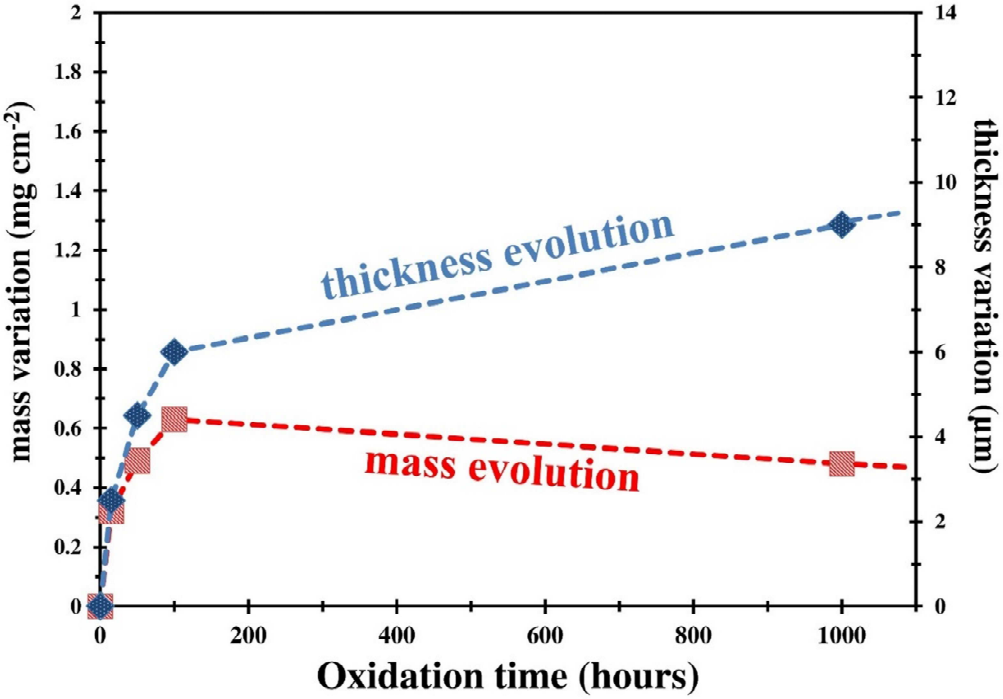
mass variation (mg cm-2)
thickness variation (µm)
thickness evolution
mass evolution
Oxidation time (hours)
0
0.2
0.4
0.6
0.8
1
1.2
1.4
1.6
1.8
2
0
2
4
6
8
10
12
14
0
200
400
600
800
1000

Fig.4

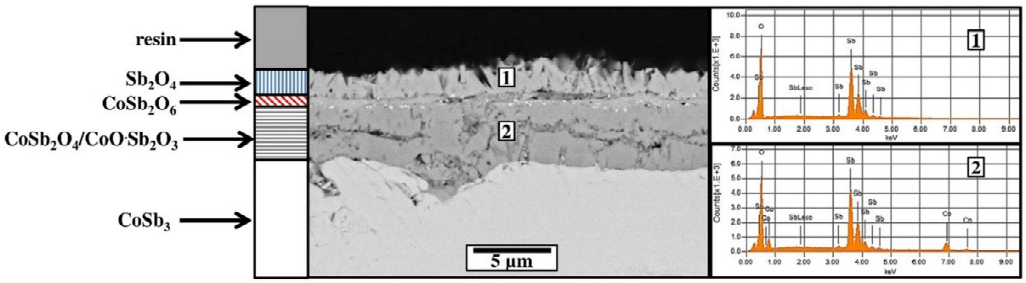

Fig.5

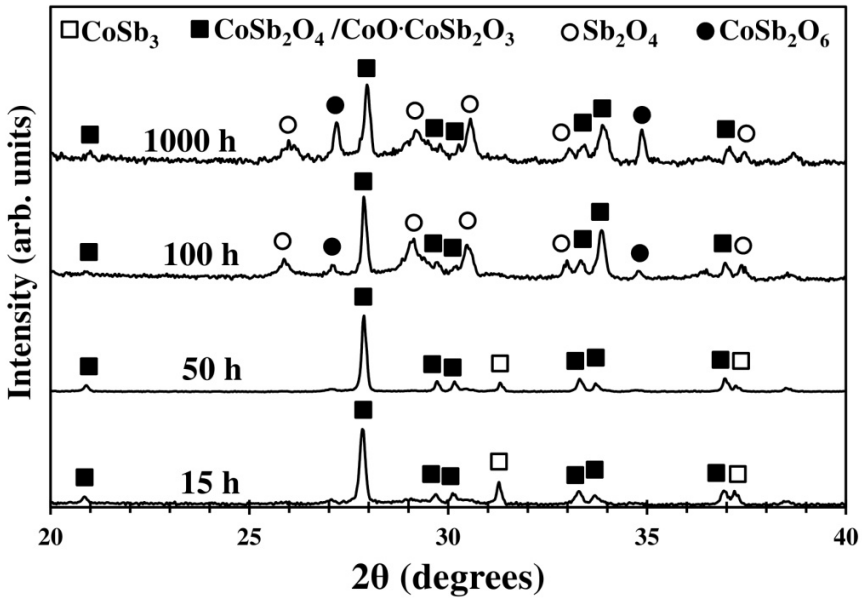
□CoSb3 ■CoSb2O4 /CoO·CoSb2O3 ○Sb2O4 ●CoSb2O6
1000 h
100 h
50 h
15 h
Intensity (arb. units)
20
25
30
35
40
2θ (degrees)

Fig.6

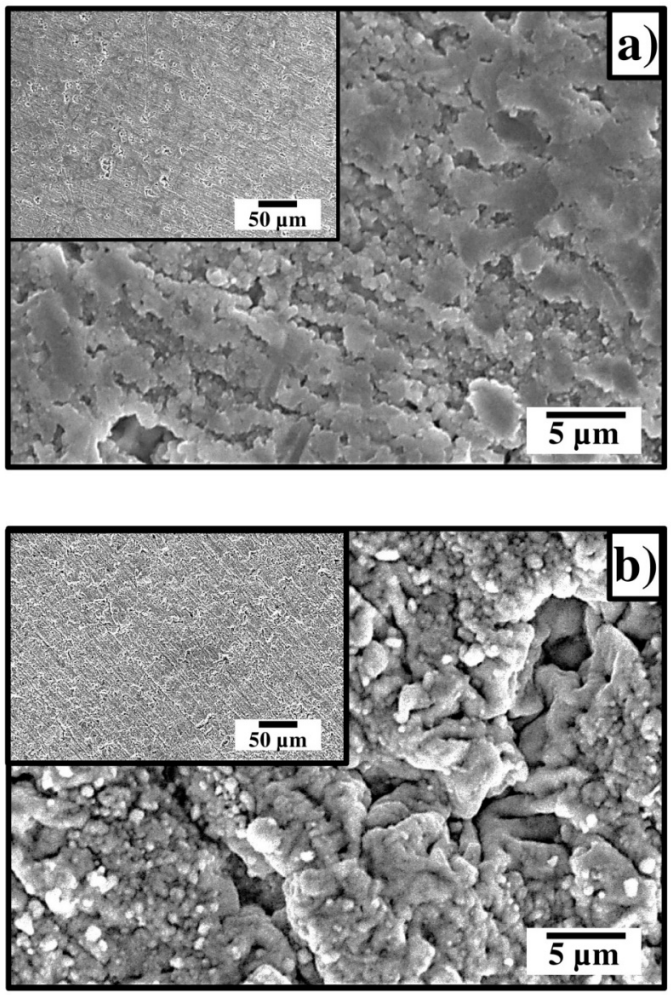

Fig.7

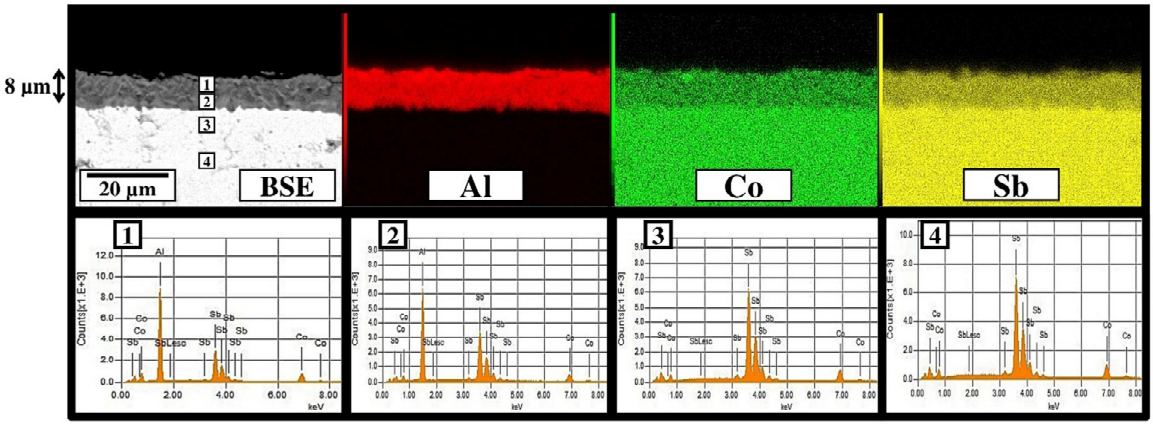

Fig.8

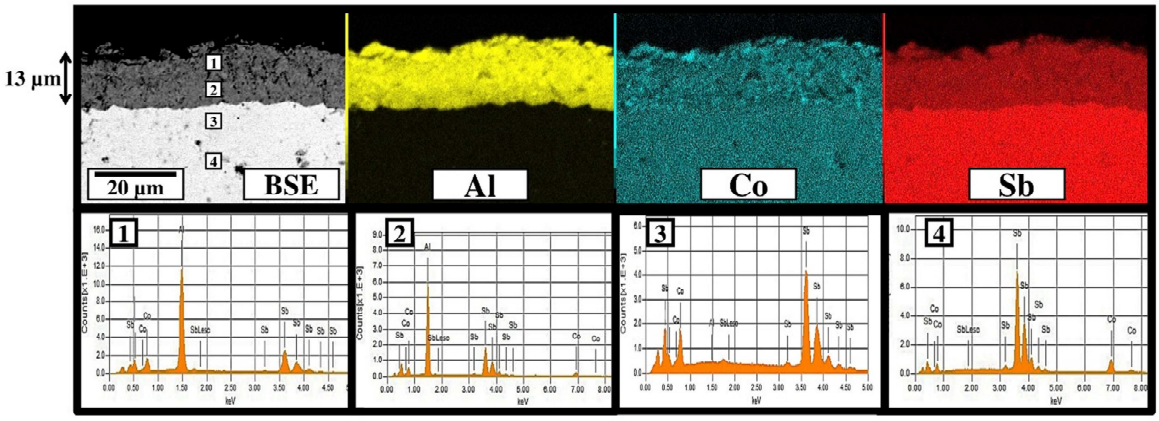

Fig.9

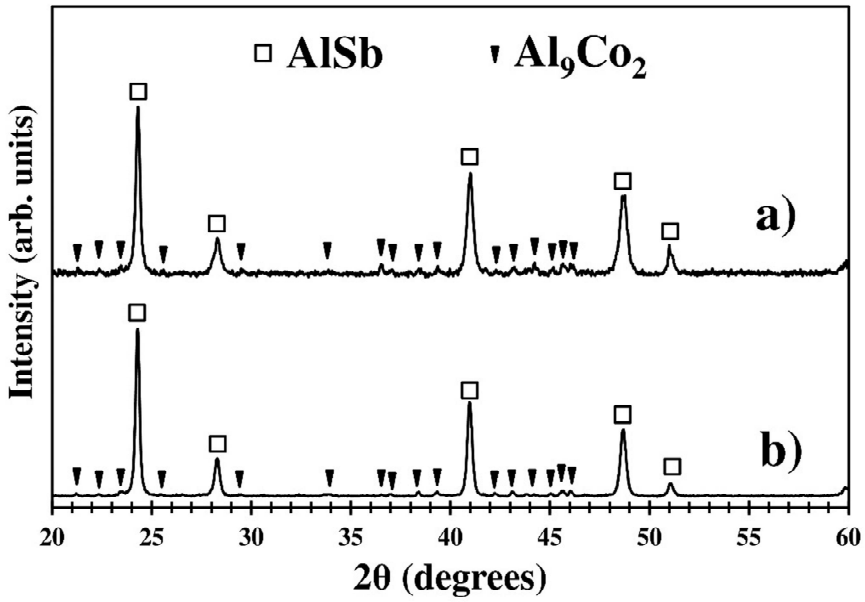
AlSb
Al9Co2
a)
b)
Intensity (arb. units)
20
25
30
35
40
45
50
55
60
2θ (degrees)

Fig.10

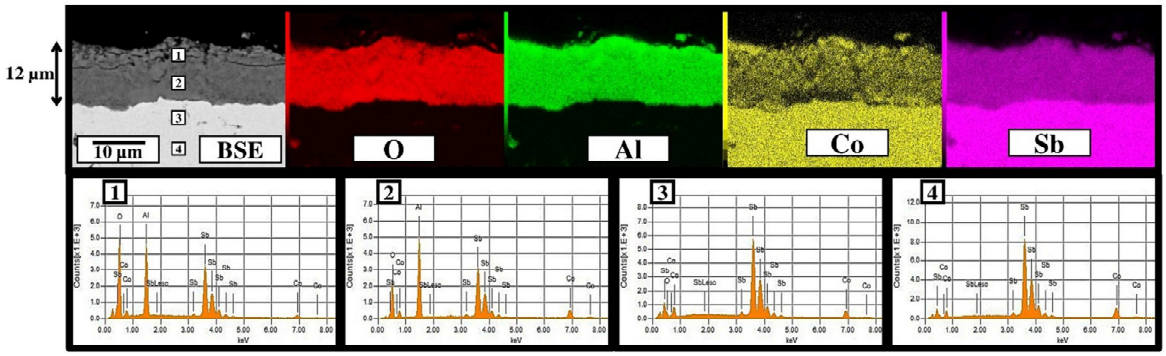

Fig.11

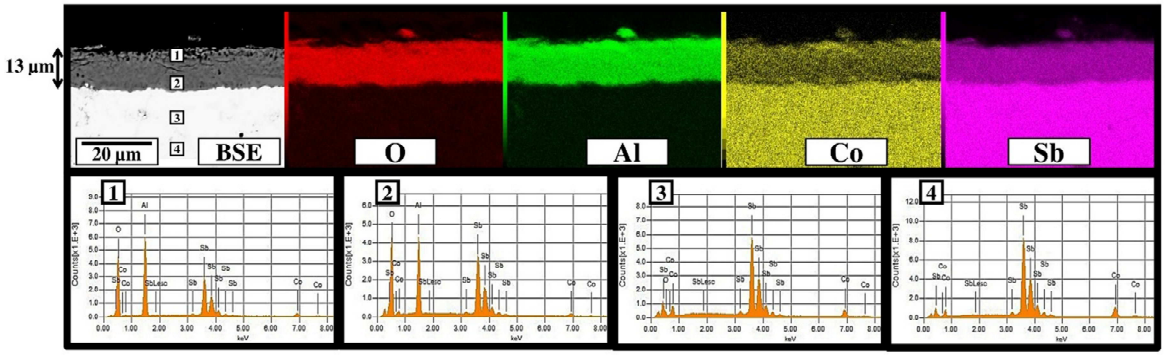

Fig.12

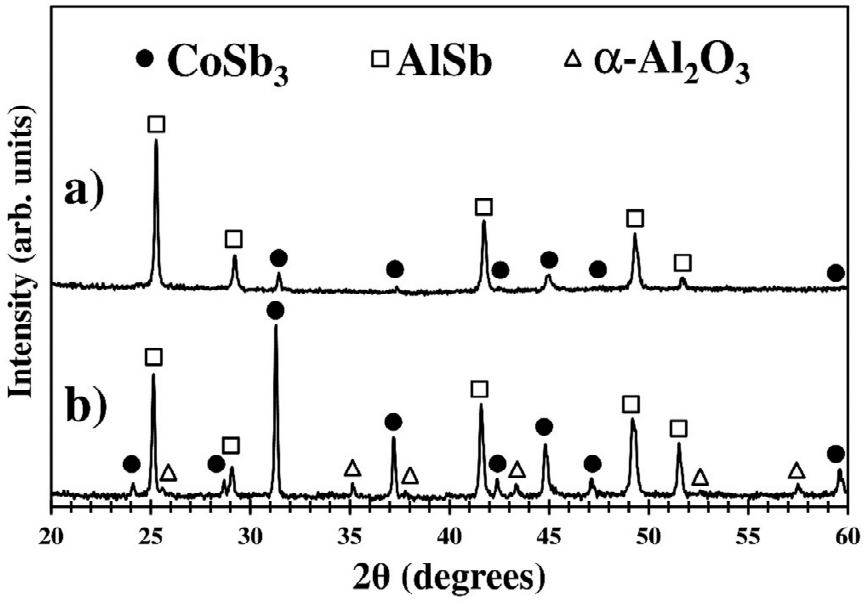
● $CoSb_3$
□ AlSb
△ α-Al_2O_3
a)
b)
Intensity (arb. units)
20
25
30
35
40
45
50
55
60
2θ (degrees)

Table 1. Elemental quantifications extracted from the EDS spectra presented in the study

	Position	at. % of O	at. % of Al	at. % of Co	at. % of Sb
Fig.4	1	62.2	-	-	37.8
	2	50.0	-	16.5	33.5
Fig.7	1	-	66.2	12.6	21.2
	2	-	59.9	10.0	30.1
	3	-	-	24.7	75.3
	4	-	-	25.2	74.8
Fig.8	1	-	68.8	12.9	18.3
	2	-	63.4	11.8	24.8
	3	-	-	25.0	75.0
	4	-	-	25.1	74.9
Fig.10	1	44.6	37.0	4.5	13.9
	2	41.0	27.6	4.6	26.8
	3	-	-	25.5	74.5
	4	-	-	24.9	75.1
Fig.11	1	46.9	38.1	4.1	10.9
	2	43.8	26.0	4.1	26.1
	3	-	-	24.7	75.3
	4	-	-	25.2	74.8

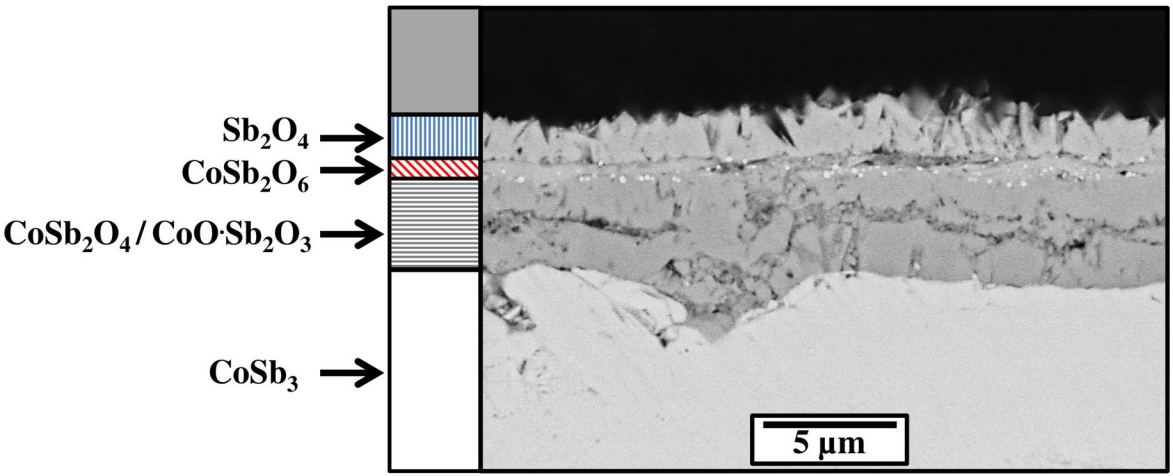
Sb_2O_4
$CoSb_2O_6$
$CoSb_2O_4$ / $CoO{\cdot}Sb_2O_3$
$CoSb_3$
5 µm